bioRxiv preprint doi: https://doi.org/10.1101/622746; this version posted April 30, 2019. The copyright holder for this preprint (which was not certified by peer review) is the author/funder, who has granted bioRxiv a license to display the preprint in perpetuity. It is made available under aCC-BY-NC-ND 4.0 International license.

Acetyl-CoA production by specific metabolites promotes cardiac repair after myocardial infarction via mediating histone acetylation

Short title: Lei et al: Epigenetic control by acetyl-CoA in heart repair

Authors: Ienglam Lei[1,2*], Shuo Tian[2*], Wenbin Gao[2*], Liu Liu[2], Yijing Guo[2], Zhong Wang[2]

[1]Faculty of Health Sciences, University of Macau, Avenida de Universidade, Taipa, Macau SAR, P.R. China
[2]Department of Cardiac Surgery, Cardiovascular Center, The University of Michigan, Ann Arbor, MI 48109, USA;

*These authors contributed equally to this study.

Addresses for Correspondence:

Zhong Wang, PhD

Department of Cardiac Surgery

Frankel Cardiovascular Research Center

University of Michigan

2800 Plymouth Road

NCRC 026-341S, Ann Arbor, MI 48109

Tel: 734-763-3691

Fax: 734-763-3697

Email: zhongw@med.umich.edu

Total word counts: 7500

bioRxiv preprint doi: https://doi.org/10.1101/622746; this version posted April 30, 2019. The copyright holder for this preprint (which was not certified by peer review) is the author/funder, who has granted bioRxiv a license to display the preprint in perpetuity. It is made available under aCC-BY-NC-ND 4.0 International license.

Abstract

Background:
We aim to connect directly the energy metabolism and epigenetics for heart therapy. Energy is fundamental for all living organisms and the heart is most sensitive to energy supply and production. One key response to energy status is to use one carbon or two carbon moieties derived from metabolites to change chromatin structure by methylation and acetylation and regulate gene expression. In particular, acetyl-CoA is a building block for energy metabolism and histone acetylation. However, the acetyl-CoA-mediated regulatory machinery integrating metabolic pathways and chromatin modifications has been under-explored in heart repair and protection.

Methods:
We conducted a screen of energy metabolites in swift production of acetyl-CoA and cardiac repair after ischemic reperfusion injury (I/R). We next examined the relationships between acetyl-CoA production, histone acetylation and heart repair after I/R. Cellular, molecular, and epigenetic studies were conducted to determine the metabolic/epigenetic network involved in executing the energy metabolite-mediated heart protection.

Results:
We identified that acetate, pyruvate, and octanoic acid (8C), but not citrate and nonanoic acid, improved heart function in I/R rats. In particular, 8C administration resulted in the most significant heart functional recovery. In a more clinically relevant setting, 8C injection at the time of reperfusion 45 minutes after left anterior descending coronary (LAD) ligation showed comparable repair effect to that of 8C administration before LAD ligation, suggesting that 8C could be a very effective metabolic natural product to treat I/R injury. Mechanistically, 8C promoted histone acetylation in cardiomyocytes (CM) after I/R injury and inhibited CM apoptosis by activating expression of anti-oxidant genes HO1, NQO1 and SOD2. We further established that the 8C-promoted histone acetylation and heart repair were carried out by metabolic enzyme medium-chain acyl-CoA dehydrogenase (MCAD) and histone acetyltransferase Kat2a.

Conclusions:
Our data demonstrate that administration of 8C dramatically improves cardiac function through metabolic acetyl-CoA-mediated histone acetylation. This study elucidates an interlinked metabolic/epigenetic network comprising 8C, acetyl-CoA, MCAD, and Kat2a in stimulating histone acetylation and anti-oxidative stress gene expression to combat heart injury. Our study provides a framework for developing novel heart repair and protection strategies at the interface of metabolism and epigenetics.

Keywords: histone acetylation, acetyl-CoA, medium chain fatty acid, ROS, crosstalk between metabolism and epigenetics, ischemic reperfusion, cardiac repair

bioRxiv preprint doi: https://doi.org/10.1101/622746; this version posted April 30, 2019. The copyright holder for this preprint (which was not certified by peer review) is the author/funder, who has granted bioRxiv a license to display the preprint in perpetuity. It is made available under aCC-BY-NC-ND 4.0 International license.

Clinical Perspective

What is New?

To our knowledge, this study represents the first systematic investigation that connects directly the energy metabolism and epigenetics for heart therapy.

Administration of octanoic acid (8C), a medium chain fatty acid, as well as a number of other metabolites, effectively protects against cardiac ischemic reperfusion (I/R) injury in rats.

8C administration quickly elevates acetyl-CoA production and promotes histone acetylation in cardiomyocyte protection against I/R injury.

8C promoted histone acetylation and heart repair is mediated by metabolic enzyme medium-chain acyl-CoA dehydrogenase (MCAD) and histone acetyltransferase Kat2a.

This study elucidates an interlinked metabolic/epigenetic network comprising 8C, acetyl-CoA, MCAD, and Kat2a in stimulating histone acetylation and anti-oxidative stress gene expression to combat heart injury.

What are the clinical implications?

Our findings provide a novel mechanism centered on acetyl-CoA linking metabolism and epigenetic regulation of gene expression in cardiomyocytes during I/R heart injury.

Natural metabolites that swiftly generate acetyl-CoA and promote histone acetylation in heart protection may have the advantage of moving into clinical practice with expedited FDA approval.

This investigation provides a framework for developing novel heart repair and protection strategies at the interface of metabolism and epigenetics.

bioRxiv preprint doi: https://doi.org/10.1101/622746; this version posted April 30, 2019. The copyright holder for this preprint (which was not certified by peer review) is the author/funder, who has granted bioRxiv a license to display the preprint in perpetuity. It is made available under aCC-BY-NC-ND 4.0 International license.

Introduction

Energy is a fundamental requirement for all living organisms and its production typically requires fuels (metabolites) and oxygen. Heart is a most sensitive organ to energy supply and production. One key response to fuel changes is the epigenetic modifications using one carbon or two carbon moieties derived from metabolites to change chromatin structure by methylation and acetylation and regulate gene expression[1]. Notably, a bi-directional interplay between metabolism and epigenetic control has been proposed recently: metabolism directly regulates chromatin epigenetic state, whereas chromatin state define gene control in response to metabolic status[2, 3].

Myocardial infarction (MI), which blocks the supply of energy to infarcted area, is one of the leading causes of death in the world[4]. Despite the severe complications of this devastating disease[5], the therapies to reduce MI injury are still limited. MI is accompanied by severe energy deprivation and extensive epigenetic changes. Regulations in either energy metabolism or epigenetics are essential for heart function and pathogenesis[6, 7], but how these two events are interlinked in the context of MI has been under-explored. Clearly, exploring an integrated metabolic and chromatin control in MI injury and heart repair and regeneration may provide novel therapies against heart injury.

Acetyl-CoA is a building block for both energy metabolism and histone acetylation. Acetyl-CoA is an evolutionarily conserved intermediate energy metabolite in TCA cycle for ATP production. Meanwhile, acetyl-CoA is the substrate for histone acetyltransferases (HATs) to transfer the acetyl-group to histone residues for histone acetylation[8, 9]. Manipulation of acetyl-CoA, either by intervention of synthetic enzymes, or nutrient source could alter histone acetylation in various cell types[9-12]. In particular, acetyl-CoA induces metabolic adaptations through regulating histone acetylation in response to starving or hypoxia conditions[13, 14]. Myocardial ischemic reperfusion (I/R) injury causes dramatic metabolism changes and subsequent histone deacetylation. Importantly, inhibition of histone deacetylation activity protects heart function after I/R injury[15-17] and inhibits cardiac remodeling and heart failure[18]. Thus, the intersection of acetyl-CoA-mediated metabolism and histone acetylation is very likely a novel hub for identifying targets for heart repair.

In this study, we set out to identify an interlinked metabolic and epigenetic network that would produce acetyl-CoA for histone acetylation and gene regulation, which could in turn promote heart repair and protection after I/R injury. We investigated various carbon sources for acetyl-CoA synthesis in heart repair. Among them, we found that octanoic acid (8C) showed most effective improvement of cardiac functions after I/R. A single IP injection of 8C at the time of reperfusion significantly reduced the infarct size and improved cardiac function at both 24 hours and 4 weeks after MI. We found that 8C produced acetyl-CoA and rescue histone acetylation after simulate ischemic reperfusion (sI/R), which led to elevated expression of anti-oxidant genes. We further established that the metabolic enzyme medium-chain acyl-CoA dehydrogenase (MCAD) and histone acetyltransferase Kat2a were key factors in transferring the acetyl moiety in 8C to acetyl groups in histone acetylation. Thus, our study established a novel interlinked metabolic/epigenetic network that may provide new strategies to treat heart injuries.

bioRxiv preprint doi: https://doi.org/10.1101/622746; this version posted April 30, 2019. The copyright holder for this preprint (which was not certified by peer review) is the author/funder, who has granted bioRxiv a license to display the preprint in perpetuity. It is made available under aCC-BY-NC-ND 4.0 International license.

Methods

Animal experiment

All experiments were approved by the Animal Care and Use Committee of the University of Michigan and were performed in accordance with the recommendations of the American Association for the Accreditation of Laboratory Animal Care.

Generation of rat I/R Models

Myocardial ischemia/reperfusion was carried out in rats as described previously[15]. Briefly, 170-180 grams male SD rats (Charlse River Laboratoires) were anaesthetized with ketamine (100 mg/kg) and xylazine (10 mg/kg). Myocardial ischemia was performed by occlusion of the left descending coronary artery (LAD) using 6-0 silk sutures. After 45 min of ischemia, the myocardium was reperfused. Acetate, pyruvate, citrate, octanoic acid (8C) or nonanoate acid (9C) was intraperitoneal (i.p.) injected to rats for 3 continuous days before MI surgery and at the onset or only 45 min after LAD occlusion.

Echocardiography

Echocardiography (ECG) was performed after surgery. Left ventricular internal diameter end diastole (LVIDd) and left ventricular internal diameter end systole (LVIDs) were measured perpendicularly to the long axis of the ventricle. Ejection fraction (EF) and fractional shortening (FS) were calculated according to LVIDd and LVIDs.

Triphenyltetrazolium chloride (TTC) staining

The hearts were frozen rapidly and sliced into five 2 mm transverse sections. The sections were incubated at 37°C with 1% TTC in phosphate buffer (pH 7.4) for 10 min, fixed in 10% formaldehyde solution, photographed and calculated using Image J software. The infarct size was expressed as a percentage of infarct volume versus left ventricle volume.

Measurement of serum CK, serum LDH and tissue SOD

Blood samples were collected at 24h after reperfusion and plasma was isolated. The creatine kinase (CK) and lactate dehydrogenase (LDH) level in plasma were measured according to the manufacturer's instructions. Ventricles were crushed to a powder using liquid nitrogen and homogenized in saline with the weight/volume ratio of 1:10. After centrifuging for 10min at 3,500 rpm, the supernatants were withdrawn for SOD measurement according to the manufacturer's instructions. Bradford protein assay was performed to determine the protein concentration.

Histology assay

Histological studies were performed as previously described[19]. Briefly, animals were sacrificed and the hearts were perfused with 20% KCl. After being fixed with zinc fixative solution (BD Pharmingen) and dehydrated by alcohol, the samples were embedded by paraffin and sectioned into 5 μm slides. The sections were processed for immunostaining, including Masson's trichrome, immunofluorescence and TUNEL assay (in situ cell death detection kit, Roche). Images were captured by Aperio (Leica Biosystems, Buffalo Grove, IL, USA) and a confocal microscope (Nikon, Melville, NY, USA) and analyzed by Image J software.

Isolation of neonatal ventricular myocytes (NRVM) and simulated ischemic reperfusion(sI/R) in vitro

NRVM were isolated from postnatal day 1 SD rats as previously described. NRVM were cultured in 5% horse serum for 2 days then changed into serum free medium. For sI/R, cells were cultured in ischemic medium[16] and subjected to hypoxia in a chamber with 94% N_2,1% O_2, 5% CO_2. After 2 hours of hypoxia, the cells were then reperfused in DMEM for 4 hours in serum free medium at 95% air and 5% CO_2 .

Measurement of Acetyl-CoA

Acetyl-CoA was measured using acetyl-CoA assay kit (biovision) according to the manufacturer's instructions. For tissues, hearts were weighted and pulverized, then subjected to 400 μL of 1M perchloric acid/100 mg tissue. For cell culture, the samples were isolated and lysed in RIPA buffer. The lysate was deproteinized by 1M perchloric acid. The deproteinized

bioRxiv preprint doi: https://doi.org/10.1101/622746; this version posted April 30, 2019. The copyright holder for this preprint (which was not certified by peer review) is the author/funder, who has granted bioRxiv a license to display the preprint in perpetuity. It is made available under aCC-BY-NC-ND 4.0 International license.

supernatant was neutralized by 3M $KHCO_3$. The supernatant was then measured acetyl-CoA following the standard kit protocol. The size of NRVM was estimated at 6000μm^3 and the concentration of acetyl-CoA in cells were calculated accordingly.

Western blot

Proteins were extracted in lysis buffer followed by centrifugation at 4°C for 15 min at 12,000 rpm. Protein concentration was measured by Bradford protein assay and 40 μg of total protein was separated by SDS-PAGE and then transferred to PVDF membranes. The membranes were blocked with 5% nonfat dry milk for 1 h at room temperature and then incubated with primary antibodies overnight at 4°C. After 3 washings with TBST, the membranes were incubated with secondary antibody in TBST solution for 1 h at room temperature. After 3 washings, the membranes were scanned and quantified by Odyssey CLx Imaging System (LI-COR Biosciences, USA).

RNA-seq

The LV tissue was collected and total RNA was extracted by Trizol following manufacture's protocol. The total RNA was treated with DNAse Turbo to remove genomic DNA. RNA quality was assessed using Agilent Bioanalyzer Nano RNA Chip. 1 μg of total RNA (RIN > 8) was used to prepare the sequencing library using NEBNext Stranded RNA Kit with mRNA selection module. The library was sequenced on illumina HiSeq 4000 (single end, 50 base pair) at the Sequencing Core of University of Michigan.

RNA-seq data analysis

RNA-seq data was quantified using Kallisto (Version 0.43.0)[20] with parameters: --single -b 100 -l 200 -s 20 using the Rnor6.0 (ensembl v91). The estimated transcript counts were exported by tximport[21] for Deseq2 analysis[22]. Differential expression was then calculated using Deseq2 default setting. Gene Ontology analysis was performed using GSEA[23].

DHE staining

For in vitro staining, 5mM of DHE solution was directly added to medium to final concentration of 5μM and cultured at 37°C for 30 minutes. The cells were washed 3 times of PBS and observed under microscope or dissociated for FACS analysis.

For in vivo staining, heart tissues were embedded in OCT immediately after harvested. Tissues were then sectioned at 20 μm. 5μM of DHE solution was directly apply to sections for 30 minutes at 37°C. After 3 washes of PBS, the sections were mounted and observed under the microscope.

ChIP

ChIP experiments were performed as previously described[24]. Cells were fixed in 1% formaldehyde and quenched with 0.125M glycine. Nuclei pellets were then harvested and digested with MNase at 37°C for 2 minutes. After brief sonication, chromatin solution was incubated with Dynabeads and antibodies against H3K9ac overnight. Beads were washed four times with LiCl wash buffer and one wash of TE buffer then eluted with elution buffer at 65°C. DNA was purified using Bioneer PCR purification kit. Enrichment of immunoprecipitated DNA was then validated by quantitative PCR.

Statistical analysis

GraphPad Prism Software (version 7) was used for statistical analysis. Data were expressed as the mean ± SD. Statistical comparisons between two groups were performed by Student's t test, and more than two groups were performed by two-way or one-way ANOVA followed by posthoc Turkey comparison. Groups were considered significantly different at $p < 0.05$.

bioRxiv preprint doi: https://doi.org/10.1101/622746; this version posted April 30, 2019. The copyright holder for this preprint (which was not certified by peer review) is the author/funder, who has granted bioRxiv a license to display the preprint in perpetuity. It is made available under aCC-BY-NC-ND 4.0 International license.

Results

Swift acetyl-CoA generating metabolites acetate, pyruvate, and octanoic acid protected heart function after I/R injury

Myocardial infarction induces dramatic metabolic and epigenetic changes including decrease of acetyl-CoA synthesis and histone acetylation[25, 26]. Consistent with this observation, we found acetyl-CoA reduction after I/R (Supplemental Figure 1) and investigated whether energy metabolites that swiftly produce acetyl-CoA could improve cardiac function after I/R. Rats subjected to I/R surgery were divided into 6 groups after ligation and i.p. injected with saline, acetate (500 mg/kg)[27], pyruvate (500 mg/kg)[28], citrate (500 mg/kg), octanoic acid (8C, 160 mg/kg)[29] and nonanoate acid (9C, 200 mg/kg)[29]. The infarct size was measured by tripheyltetrazolium chloride (TTC) staining at 24 hours after I/R (Figure 1A). Surprisingly, these carbon sources displayed distinct effects on reducing myocardial infarct size. Among the five metabolites examined, acetate, pyruvate and 8C significantly reduced the infarct size, whereas citrate and 9C treatment did not reduce the infarct size compared to saline treated groups (Figure 1B-1C). These results indicated a potential beneficial effect of replenishment of acetyl-CoA with specific metabolites for heart repair after I/R.

Administration of 8C at reperfusion improved short-term and long-term cardiac function after I/R

Because 8C administration resulted in the most dramatic protection among all the metabolites tested after I/R (Figure 1B-1C), we focused on investigating the role of 8C on heart protection in the following studies. To mimic a more clinical relevant setting, we next i.p. injected 8C (160 mg/kg) or saline at the time of reperfusion after 45 minutes of LAD ligation (Figure 1D). TTC staining showed that 24 hours after reperfusion, 8C treatment led to approximately 50% reduction of infarct size compared to saline control (Figure 1E-1F). Moreover, 8C also significantly improved the left ventricle function evaluated by echocardiography 24 hours after I/R. Compared to saline treated rats, the EF and FS increased from 46% to 57% and 24% to 31%, respectively (Figure 1G-1H), while the normal rat heart has EF at 72% and FS at 42%. These results indicated that 8C significantly improve cardiac function by approximately 40%. To investigate whether a single dose of 8C administration is beneficial for long-term cardiac function after I/R, we examined the infarct size and heart function at 4 weeks after I/R. Trichrome Masson staining showed that the infarct size was notably reduced after 8C treatment (Figure 1I-1J). The left ventricle function was also improved after 8C treatment as evidenced by the increase of EF and FS (Figure 1K-1L). Altogether, our results indicated that 8C administration at the time of reperfusion significantly improved both short-term and long-term cardiac function after I/R.

8C attenuated cardiomyocyte apoptosis through alleviating oxidative stress.

Apoptosis is one of the major reasons for cardiac damage after I/R injury[30]. To detect the impact of 8C on cardiomyocyte apoptosis, TUNEL was performed at the border zone of I/R hearts. 8C treatment dramatically reduced TUNEL positive cardiomyocytes in border zone (Figure 2A-2B). Consistent with the TUNEL assay, the protein levels of cell death indicators serum CK and LDH were also reduced in I/R rats after 8C administration (Figure 2C-2D). Moreover, 8C led to reduction in pro-apoptotic regulator Bax and upregulation of anti-apoptotic gene Bcl2 at 24 hours after I/R injury (Figure 2E). To study the mechanism of the beneficial effect of 8C after I/R, we examined the gene expression profile at border zone 24 hours after I/R by RNA-seq. GSEA[23] showed that genes involved in apoptotic signaling pathways were enriched in saline-

bioRxiv preprint doi: https://doi.org/10.1101/622746; this version posted April 30, 2019. The copyright holder for this preprint (which was not certified by peer review) is the author/funder, who has granted bioRxiv a license to display the preprint in perpetuity. It is made available under aCC-BY-NC-ND 4.0 International license.

treated compared to 8C-treated rats after I/R (Figure 2F). Specifically, I/R reduced the expression of anti-oxidative stress enzymes such as SOD1, SOD2, SOD3 and CAT, while 8C restored the expression of these genes (Figure 2G). Since I/R induced oxidative stress triggers CM apoptosis after reperfusion[31], it is likely that 8C reduced cell death by activating anti-oxidant process after I/R injury. To address this, we measured the level of cardiac reactive oxygen species (ROS) after I/R by staining of dihydroethidium (DHE), a chemical that could be oxidized by ROS[32]. The intensity of DHE signal was significantly lower in the presence of 8C after I/R (Figure 2H-2I), indicating that 8C reduced oxidative stress after I/R. Moreover, 8C rescued the myocardial SOD activity after I/R (Supplemental Figure 2). Altogether, these results showed that one major mechanism through which 8C improved cardiac function after I/R was to reduce the oxidative stress and subsequent cell apoptosis.

To further investigate the effect of 8C on oxidative stress and apoptosis in cardiomyocytes, neonatal rat ventricle myocytes (NRVM) were subjected to simulate ischemic reperfusion[16] (sI/R) with or without 8C. NRVM were pretreated with 8C or PBS for 12 hours, and then subjected to 2 hours of simulated ischemia followed by 4 hours of simulated reperfusion. The percentage of apoptotic cells after sI/R was measured by labeling with Annexin V and PI. 8C significantly reduced the percentage of apoptosis cells, as evidenced by the lower percentage of Annexin V and PI double positive cells (Figure 3A-3B). In addition, combination of CCK8 and LDH release assays were used to measure the total cell death[33]. 8C led to reduced cell death after sI/R as showed by increased cell viability and decreased LDH release into to culture medium (Figure 3C-3D). Moreover, 8C reduced the expression of cleaved Caspase 3 after sI/R. Consequently, the expression of cleaved PARP, which is cleaved by Caspase 3 was also reduced with 8C administration (Figure 3E). Altogether, these results demonstrated that 8C reduced the apoptosis of NRVM exposed to sI/R. To assess whether 8C reduced the oxidative stress in cardiomyocytes after sI/R, the accumulation of ROS level was measured by the intensity of DHE staining. The ROS levels were significantly decreased in NRVM with 8C treatment after sI/R (Figure 3F-3H), indicating a direct effect of 8C in alleviating oxidative stress after sI/R. Thus, our collective in vivo and in vitro results revealed that 8C attenuated cardiomyocyte apoptosis through alleviating oxidative stress.

Increasing acetyl-CoA synthesis by 8C administration activated anti-oxidant genes through stimulating histone acetylation after I/R injury.

8C can quickly enter into cells and become oxidized to generate cytosolic acetyl-CoA[34] and contribute to histone acetylation in several cell types[12], and histone acetylation plays an important role in regulating cellular response to oxidative stress[35]. We therefore hypothesized that 8C protected cardiomyocytes against I/R injury through stimulating histone acetylation. We first measured the acetyl-CoA level after I/R injury in vivo and in vitro. I/R injury induced a reduction of acetyl-CoA level in both heart and NRVM, while 8C significantly increased the production of acetyl-CoA in heart and NRVM (Figure 4A-4B). To determine the effect of acetyl-CoA replenishment on histone acetylation, we measured H3K9ac, H3K14ac, H3K27ac and total H3 acetylation in NRVM after sI/R. We found that sI/R led to a remarkable decrease of H3K9ac, H3K14ac, H3K27ac and acH3, and that 8C increased histone acetylation in normal NRVM and rescued sI/R reduced histone acetylation (Figure 4C-4F). These results indicated that acetyl-CoA production by 8C rescued histone acetylation decrease after sI/R.

Acetyl-CoA is the substrate for histone acetyltransferases (HATs) to generate histone acetylation by transferring the acetyl-group from acetyl-CoA to histone lysine residues[36]. Specifically, HATs with low affinity to acetyl-CoA are more sensitive to acetyl-CoA abundance. H3K9ac has been reported as the histone acetylation most sensitive to acetyl-CoA levels[36].

bioRxiv preprint doi: https://doi.org/10.1101/622746; this version posted April 30, 2019. The copyright holder for this preprint (which was not certified by peer review) is the author/funder, who has granted bioRxiv a license to display the preprint in perpetuity. It is made available under aCC-BY-NC-ND 4.0 International license.

Consistent with this finding, we found that 8C led to most significant changes in H3K9ac after sI/R. Thus, we reasoned that H3K9ac, which is enriched in promoters for gene activation, is one key epigenetic event for gene regulation after sI/R. To examine the potential epigenetic regulation of 8C derived acetyl-CoA in anti-oxidative stress, we performed ChIP to measure H3K9ac at the promoters of antioxidant genes. While sI/R led to increased H3K9ac level at the promoters of NQO1, HO1 and SOD2, 8C further elevated H3K9ac on the promoters of these genes (Figure 4G-4I). Consequently, 8C upregulated the expression of anti-oxidant genes including HO1, NQO1, and SOD2 after sI/R (Fig 4J-4K). Thus, these results showed an epigenetic regulation of antioxidant genes by 8C-produced acetyl-CoA.

MCAD was required for the conversion of 8C into acetyl-CoA and subsequent histone acetylation increase and heart protection

To ascertain whether 8C produced acetyl-CoA was important for the rescue of histone acetylation after sI/R, we knocked down MCAD (Supplemental Figure 3A), a key enzyme in the generation of acetyl-CoA from 8C[37]. Knockdown of MCAD disrupted the metabolism of 8C, and therefore led to reduction of histone acetylation promoted by 8C in NRVM in both normoxia and sI/R condition (Figure 5A). Thus, these data indicated that metabolic production of acetyl-CoA from 8C was required for the 8C-mediated histone acetylation regulation. To determine whether acetyl-CoA mediated histone acetylation was key to the 8C heart protective effect after I/R, we examined the cardiomyocyte survival after MCAD knockdown with and without 8C after sI/R. MCAD knockdown significantly blocked the protective effect of 8C after sI/R, as evidenced by decreased cell viability and increased LDH release in MCAD knockdown cells with 8C treatment after sI/R (Figure 5B and Supplemental Figure 3B). Importantly, MCAD knockdown blocked the 8C-reduced cellular ROS level after sI/R (Figure 5C-5D and Supplemental Figure 3C). Specifically, we found that MCAD knockdown blocked 8C stimulated H3K9ac increase in the promoters of HO1 and NQO1 after sI/R (Figure 5E-5F). Subsequently, MCAD knockdown reduced 8C-elevated expression of HO1 and NQO1 after sI/R (Figure 5G). Thus, these results demonstrated that MCAD-mediated 8C metabolism was essential for histone acetylation and attenuating apoptosis through anti-oxidant process.

HAT enzyme Kat2a was required for 8C mediated histone acetylation to inhibit oxidative stress in heart protection

HATs are the very enzymes that catalyze histone acetylation by transferring the acetyl-group from acetyl-CoA to histone lysine residues. As H3K9ac is most sensitive to physiological acetyl-CoA levels, we then hypothesized that HATs that acetylate H3K9 and are most responsive to physiological acetyl-CoA concentrations would play important roles in the cardioprotection of 8C. Kat2a and Kat2b are the major HATs that modulate H3K9ac[38]. Kat2a is mostly responsive to acetyl-CoA concentrations at 0-10 μM[39], while Kat2b is response to acetyl-CoA from 0 to 300 μM[40]. Considering the fact that acetyl-CoA levels in NRVM ranged from 1-7 μM under sI/R (Figure 4B), we focused on studying the effect of Kat2a knockdown on the protective role of 8C after sI/R. Kat2a knockdown largely abolished the H3K9ac increase caused by 8C treatment in NRVM (Figure 6A and Supplemental Figure 4A), indicating that Kat2a was a key HAT to mediate 8C-stimulated histone acetylation. Furthermore, Kat2a knockdown led to a significant decrease of cell viability and increase of LDH release (Figure 6B and Supplemental Figure 4B), suggesting that Kat2a was required for the protective effect of 8C. Moreover, knockdown of Kat2a abolished 8C's effect on inhibiting the cellular ROS level after sI/R (Figure 6C-6D and Supplemental Figure 4C). Specifically, Kat2a knockdown abolished 8C-stimulated H3K9ac increase at the promoters of HO1 and NQO1 after sI/R (Figure 6E-6F). Subsequently, Kat2a knockdown reduced 8C-elevated expression of HO1 and NQO1 after sI/R (Figure 6G). These

bioRxiv preprint doi: https://doi.org/10.1101/622746; this version posted April 30, 2019. The copyright holder for this preprint (which was not certified by peer review) is the author/funder, who has granted bioRxiv a license to display the preprint in perpetuity. It is made available under aCC-BY-NC-ND 4.0 International license.

results illustrated that Kat2a was required to execute the rescuing role of 8C after sI/R by modulating histone acetylation, which in turn activated antioxidant gene expression and attenuated cellular apoptotic after sI/R. Together our investigation revealed an integrated metabolic and epigenetic network comprising 8C, acetyl-CoA, MCAD, and Kat2a, that likely played an essential role in combating heart injury after I/R.

bioRxiv preprint doi: https://doi.org/10.1101/622746; this version posted April 30, 2019. The copyright holder for this preprint (which was not certified by peer review) is the author/funder, who has granted bioRxiv a license to display the preprint in perpetuity. It is made available under aCC-BY-NC-ND 4.0 International license.

Discussion

In this study, we have established an interlinked metabolic and epigenetic network comprising 8C, acetyl-CoA, MCAD, and Kat2a that stimulates histone acetylation and anti-oxidative stress gene expression to combat heart injury. We have screened various carbon sources that could produce acetyl-CoA, a central metabolite in energy metabolism, and shown that replenishment of acetyl-CoA significantly improves cardiac function after I/R injury. Specifically, we have demonstrated that induction of acetyl-CoA synthesis by acetate, pyruvate, and 8C metabolism stimulates histone acetylation and promotes cardiomyocyte survival after ischemic reperfusion. Our study further reveals that 8C-stimulated histone acetylation leads to increase of antioxidant gene expression for heart repair. Moreover, MCAD knockdown diminishes the 8C-induced acetylation and subsequently lowers antioxidant activity after sI/R in vitro, indicating that the metabolic conversion of 8C to acetyl-CoA is mainly responsible for histone acetylation and subsequent heart repair effect. Furthermore, the effect of 8C on heart repair through acetyl-CoA and subsequent nuclear histone acetylation is evidenced by Kat2a studies, as Kat2a knockdown largely diminishes the protective effect of 8C after sI/R. Our study demonstrates systematically for the first time that modulating acetyl-CoA abundance can determine cardiomyocyte response to I/R injury via common metabolic and epigenetic mechanisms.

Our study reveals a novel mechanism centered on acetyl-CoA that connects metabolic dynamics and epigenetic regulation in cardiac repair after I/R injury, and suggests that acetyl-CoA could be a survival signal for cardiomyocyte after I/R injury. Our data show that I/R injury reduces the cellular acetyl-CoA level, which is associated with decrease of histone acetylation and increase of cardiomyocyte death after I/R injury[26]. We further show that these associations are causally related. Administration of acetyl-CoA precursors acetate, pyruvate, and 8C significantly reduces heart damage after I/R injury. In particular, we demonstrate that 8C restores the acetyl-CoA level and subsequently increases the histone acetylation and improves cardiac function after injury. Moreover, knockdown of 8C metabolic enzyme MCAD diminishes the rescuing effect of 8C treatment. Our study is consistent with the suggestions that acetyl-CoA provides growth signals for tumor cells and yeast under nutrient stress[8] and that acetyl-CoA could serve as second messenger to modulate epigenetic response to environmental changes[2].

Our study indicates that histone acetylation is a major downstream event of 8C and acetyl-CoA in heart repair after injury. Knockdown of Kat2a, a major HAT enzyme in catalyzing histone acetylation, greatly diminishes the cardiomyocyte protective effect of 8C metabolism. Consistent with this notion, 8C effect on elevating histone acetylation is largely abolished under Kat2a knockdown conditions. Histone acetylation as a general epigenetic regulatory mechanism can play essential roles in numerous cellular processes[41]. In this study, we have identified that 8C-mediated histone acetylation increases the expression of HO1, NQO1 and SOD2 and decreases the ROS level after I/R injury in both in vivo and in vitro. These data indicate that the rescuing effect of 8C treatment after heart injury is at least partially through stimulating gene expression against oxidative stress, which is consistent with the previous observation that a high level of histone acetylation activates gene expression against oxidative stress[35]. A future genome-wide study will provide a complete picture of 8C mediated cellular processes in combating heart injury.

Histone acetylation can also be regulated by HDACs[41]. Interestingly, studies by us and others reveal that chemical inhibition of HDACs also leads to attenuation of myocardial infarction[15, 16] and heart failure[18]. Our recent work indicates that valproic acid, an FDA approved HDAC inhibitor for bipolar treatment, protects heart function after I/R injury by promoting a Foxm1-mediated transcriptional pathway[15]. In addition, SAHA, another HDAC inhibitor, blunts

bioRxiv preprint doi: https://doi.org/10.1101/622746; this version posted April 30, 2019. The copyright holder for this preprint (which was not certified by peer review) is the author/funder, who has granted bioRxiv a license to display the preprint in perpetuity. It is made available under aCC-BY-NC-ND 4.0 International license.

myocardial infarction via regulating autophagy activities[16]. Moreover, HDACi could alter the acetylation of myofibrils and govern diastolic function of heart[18]. Whether acetyl-CoA mediated histone acetylation and HDAC inhibition share the same regulatory mechanisms in cardiac repair requires detailed investigation. It will be also interesting to determine how metabolism mediated histone acetylation and HDAC inhibition coordinate their actions in cardiac repair.

Our establishment of direct connection between epigenetic status and metabolite abundance in heart repair may provide an alternative perspective for numerous published studies. For instance, activation of AMPK shows cardioprotective effect after I/R injury[42]. It is postulated that the ability of AMPK in enhancing glucose uptake[42] and suppressing ribosome biogenesis[43] is the major reason for cardioprotection. However, the translation of AMPK activation for cardiac therapy has not been successful, partially due to unknown mechanism of AMPK protection. A recent study shows that activation of AMPK results in increased level of acetyl-CoA and therefore likely elevates histone acetylation[44]. Thus, it is possible that AMPK promotes cardiac repair via direct epigenetic regulation. Similarly, altering the levels of different metabolites show beneficial effect on cardiac repair[45, 46]. Considering the potential roles of these metabolites in epigenetic regulations, re-examining these studies will likely provide new insights into manipulating metabolites to alter epigenetics in heart disease treatment, and lead to more successful therapy.

Although increasing histone acetylation by metabolic acetyl-CoA production is an effective strategy for heart repair, not all metabolites that generate acetyl-CoA and histone acetylation have the same beneficial effect. One major reason could be that certain metabolites also generate other signals that cancel or even out-weight this beneficial effect. For example, several metabolites, such as succinate, are found to be the major source of ROS production after I/R, and therefore, succinate administration aggravates I/R injury[47, 48]. 9C produces succinate through anaplerotic reaction, and our results show that the accumulation of succinate level is much higher in 9C compared to 8C treatment (Supplemental Figure 5). These data may explain the null effect of 9C and possibly citrate administration in heart repair. Overall, this study elucidates that exploring detailed metabolic and epigenetic mechanisms mediated by various metabolic carbon sources in combating I/R injury will be an exciting research area to develop potential effective heart therapies.

bioRxiv preprint doi: https://doi.org/10.1101/622746; this version posted April 30, 2019. The copyright holder for this preprint (which was not certified by peer review) is the author/funder, who has granted bioRxiv a license to display the preprint in perpetuity. It is made available under aCC-BY-NC-ND 4.0 International license.

Funding sources

This work was supported by National Institutes of Health (NIH) of United States (1R01HL109054), an Inaugural Grant from the Frankel Cardiovascular Center, an MCube Grant from University of Michigan, and a Pilot Grant from the University of Michigan Health System – Peking University Health Sciences Center Joint Institute for Clinical and Translational Research.

bioRxiv preprint doi: https://doi.org/10.1101/622746; this version posted April 30, 2019. The copyright holder for this preprint (which was not certified by peer review) is the author/funder, who has granted bioRxiv a license to display the preprint in perpetuity. It is made available under aCC-BY-NC-ND 4.0 International license.

Figure Legends

Figure 1. 8C administration attenuates ischemia-reperfusion injury in rats. (A) Schematic diagram of different carbon source administration prior to I/R surgery. (B) Representative figures of heart sections at 24 hours after I/R in presence of different metabolites. Scale bar: 2.5 mm. (C) Quantification of infarct size by Image J. (D) Schematic diagram of 8C administration post ischemic injury. (E) Representative figures of heart sections at 24 hours after I/R with or without 8C administration at reperfusion after 45 minutes ischemic. Scale bar: 2.5 mm (F) Quantification of infarct size in figure 1E. (G-H) LV ejection fraction and fractional shortening at 24 hours after I/R. (I) Trichrome masson staining of heart section after 4 weeks of I/R. (J) Quantification of infarct size in figure 1I. (K-L) LV ejection fraction and fractional shortening at 4 weeks after I/R. Error bars represent S.D. n=5, * p<0.05, **p<0.01, vs I/R group. $^{\#}$p<0.05, vs sham group.

Figure 2. Post ischemic administration of 8C reduces the oxidative stress and cell death after I/R injury. (A) Representative of TUNEL and cTnT double staining at boarder zone at 24 hours post I/R injury. Scale bar: 100 μm (B) Quantification of cardiomyocytes cell death of 12 sections (C-D) Serum CK and LDH level at 24 hours post I/R. (E) Western blot of Bax and Bcl2 at 24 hours after I/R. (F) Gene ontology analysis of apoptotic pathways after I/R with and without 8C treatment. (G) Heatmap of anti-oxidant genes. (H) ROS levels were evaluated by DHE staining. Scale bar: 200μm. (I) Relative mean DHE fluorescent intensity measure by Image J. Error bars represent S.D. n=4. *p<0.05, **p<0.01 vs Sham; $^{\#}$p<0.05, $^{\#\#}$p<0.01 vs I/R group.

Figure 3. 8C attenuates NRVM apoptosis through reducing oxidative stress. (A) FACS analysis of Annexin V and PI staining in NRVM exposed to sI/R with and without 8C treatment. (B) Quantification of percentage of Annexin V+ and PI + cells. Cell viability and cell death measurement in NRVM with sI/R using CCK8 detection kit (C) and LDH assay kit (D). (E) Western blot of cleaved Caspase 3 and cleaved PARP in NRVM after sI/R treatment. (F) NRVM cellular ROS levels are indicated by DHE staining after sI/R treatment. Scale bar: 200μm (G) FACS analysis of DHE staining NRVM after sI/R. (H) Relative mean fluorescence intensity of DHE staining. n=3, **p<0.01, ***p<0.001, vs Normoxia+PBS; $^{\#\#}$ p<0.01, $^{\#\#\#}$p<0.001 vs sI/R+PBS.

Figure 4. 8C stimulates histone acetylation and promotes antioxidant gene expression. (A) Quantification of Acetyl-CoA levels in sham and I/R rats at indicated conditions. (B) Quantification of Acetyl-CoA concentrations in NRVM subjected to sI/R. (C-F) 8C rescues sI/R reduced H3K9ac, H3K27ac, H3K14ac and total acH3 levels. NRVMs were treated with or without 0.5mM 8C under sI/R. The histone acetylation levels were determined by western blot. Total H3 in the same blot was used as loading control. (G-I) Quantification of H3K9ac at promoters of HO1, NQO1, and SOD2 at indicated conditions. (J-K) Western blot and quantifications of HO1, NQO1, and SOD2 in NRVM after sI/R. n=3, *p<0.01, **p<0.01, ***p<0.001, vs Normoxia+PBS; $^{\#}$p<0.05, $^{\#\#}$p<0.01 vs sI/R+PBS.

Figure 5. MCAD was required for the conversion of 8C into acetyl-CoA and subsequent histone acetylation increase and heart protection. (A) Western blot of H3K9ac level showed MCAD knockdown reduced 8C-induced H3K9ac increase in NRVM under both normoxia and sI/R. (B) Measurement of medium LDH level in NRVM at indicated condition using LDH assay kit. (C) FACS analysis of DHE staining NRVM after sI/R. (D) Relative mean fluorescence intensity of DHE staining. (E-F) Quantification of H3K9ac at promoters of HO1 and NQO1 after sI/R at indicated conditions. (G) Western blot of HO1 and NQO1 in NRVM after sI/R. n=3, *p<0.05, ***p<0.001, vs Normoxia+PBS+shCTL; $^{\#}$p<0.05, $^{\#\#}$p<0.01, $^{\#\#\#}$p<0.001 vs sI/R+PBS+shCTL.

bioRxiv preprint doi: https://doi.org/10.1101/622746; this version posted April 30, 2019. The copyright holder for this preprint (which was not certified by peer review) is the author/funder, who has granted bioRxiv a license to display the preprint in perpetuity. It is made available under aCC-BY-NC-ND 4.0 International license.

Figure 6. HAT enzyme Kat2a was required for 8C mediated histone acetylation to inhibit oxidative stress in heart protection. (A) Western blot of H3K9ac level showed Kat2a knockdown reduced 8C-induced H3K9ac increase in NRVM under both normoxia and sI/R. (B) Measurement of medium LDH level in NRVM at indicated condition using LDH assay kit. (C) FACS analysis of DHE staining NRVM after sI/R. (D) Relative mean fluorescence intensity of DHE staining. (E-F) Quantification of H3K9ac at promoters of HO1 and NQO1 after sI/R at indicated conditions. (G) Western blot of HO1 and NQO1 in NRVM after sI/R. n=3, *p<0.05, **p<0.01, ***p<0.001, vs Normoxia+PBS+shCTL; $^{\#}$p<0.05, $^{\#\#}$p<0.01, $^{\#\#\#}$p<0.001 vs sI/R+PBS+shCTL.

bioRxiv preprint doi: https://doi.org/10.1101/622746; this version posted April 30, 2019. The copyright holder for this preprint (which was not certified by peer review) is the author/funder, who has granted bioRxiv a license to display the preprint in perpetuity. It is made available under aCC-BY-NC-ND 4.0 International license.

Reference:

1. Reid MA, Dai Z and Locasale JW. The impact of cellular metabolism on chromatin dynamics and epigenetics. *Nat Cell Biol*. 2017;19:1298-1306.
2. Pietrocola F, Galluzzi L, Bravo-San Pedro JM, Madeo F and Kroemer G. Acetyl coenzyme A: a central metabolite and second messenger. *Cell Metab*. 2015;21:805-21.
3. Shi L and Tu BP. Acetyl-CoA and the regulation of metabolism: mechanisms and consequences. *Curr Opin Cell Biol*. 2015;33:125-31.
4. Pagidipati NJ and Gaziano TA. Estimating deaths from cardiovascular disease: a review of global methodologies of mortality measurement. *Circulation*. 2013;127:749-56.
5. Ibanez B, Heusch G, Ovize M and Van de Werf F. Evolving therapies for myocardial ischemia/reperfusion injury. *J Am Coll Cardiol*. 2015;65:1454-71.
6. Keating ST and El-Osta A. Epigenetics and metabolism. *Circ Res*. 2015;116:715-36.
7. Maack C and Murphy E. Metabolic cardiomyopathies - fighting the next epidemic. *Cardiovasc Res*. 2017.
8. Cai L, Sutter BM, Li B and Tu BP. Acetyl-CoA induces cell growth and proliferation by promoting the acetylation of histones at growth genes. *Mol Cell*. 2011;42:426-37.
9. Wellen KE, Hatzivassiliou G, Sachdeva UM, Bui TV, Cross JR and Thompson CB. ATP-citrate lyase links cellular metabolism to histone acetylation. *Science*. 2009;324:1076-80.
10. Sutendra G, Kinnaird A, Dromparis P, Paulin R, Stenson TH, Haromy A, Hashimoto K, Zhang N, Flaim E and Michelakis ED. A nuclear pyruvate dehydrogenase complex is important for the generation of acetyl-CoA and histone acetylation. *Cell*. 2014;158:84-97.
11. Zhao S, Torres A, Henry RA, Trefely S, Wallace M, Lee JV, Carrer A, Sengupta A, Campbell SL, Kuo YM, Frey AJ, Meurs N, Viola JM, Blair IA, Weljie AM, Metallo CM, Snyder NW, Andrews AJ and Wellen KE. ATP-Citrate Lyase Controls a Glucose-to-Acetate Metabolic Switch. *Cell Rep*. 2016;17:1037-1052.
12. McDonnell E, Crown SB, Fox DB, Kitir B, Ilkayeva OR, Olsen CA, Grimsrud PA and Hirschey MD. Lipids Reprogram Metabolism to Become a Major Carbon Source for Histone Acetylation. *Cell Rep*. 2016;17:1463-1472.
13. Bulusu V, Tumanov S, Michalopoulou E, van den Broek NJ, MacKay G, Nixon C, Dhayade S, Schug ZT, Vande Voorde J, Blyth K, Gottlieb E, Vazquez A and Kamphorst JJ. Acetate Recapturing by Nuclear Acetyl-CoA Synthetase 2 Prevents Loss of Histone Acetylation during Oxygen and Serum Limitation. *Cell Rep*. 2017;18:647-658.
14. Gao X, Lin SH, Ren F, Li JT, Chen JJ, Yao CB, Yang HB, Jiang SX, Yan GQ, Wang D, Wang Y, Liu Y, Cai Z, Xu YY, Chen J, Yu W, Yang PY and Lei QY. Acetate functions as an epigenetic metabolite to promote lipid synthesis under hypoxia. *Nat Commun*. 2016;7:11960.
15. Tian S, Lei I, Gao W, Liu L, Guo Y, Creech J, Herron TJ, Xian S, Ma PX, Eugene Chen Y, Li Y, Alam HB and Wang Z. HDAC inhibitor valproic acid protects heart function through Foxm1 pathway after acute myocardial infarction. *EBioMedicine*. 2019;39:83-94.
16. Xie M, Kong Y, Tan W, May H, Battiprolu PK, Pedrozo Z, Wang ZV, Morales C, Luo X, Cho G, Jiang N, Jessen ME, Warner JJ, Lavandero S, Gillette TG, Turer AT and Hill JA. Histone deacetylase inhibition blunts ischemia/reperfusion injury by inducing cardiomyocyte autophagy. *Circulation*. 2014;129:1139-51.

bioRxiv preprint doi: https://doi.org/10.1101/622746; this version posted April 30, 2019. The copyright holder for this preprint (which was not certified by peer review) is the author/funder, who has granted bioRxiv a license to display the preprint in perpetuity. It is made available under aCC-BY-NC-ND 4.0 International license.

17. Weeks KL. HDAC inhibitors and cardioprotection: Homing in on a mechanism of action. *EBioMedicine*. 2019;40:21-22.
18. Jeong MY, Lin YH, Wennersten SA, Demos-Davies KM, Cavasin MA, Mahaffey JH, Monzani V, Saripalli C, Mascagni P, Reece TB, Ambardekar AV, Granzier HL, Dinarello CA and McKinsey TA. Histone deacetylase activity governs diastolic dysfunction through a nongenomic mechanism. *Sci Transl Med*. 2018;10.
19. Li Y, Tian S, Lei I, Liu L, Ma P and Wang Z. Transplantation of multipotent Isl1+ cardiac progenitor cells preserves infarcted heart function in mice. *American journal of translational research*. 2017;9:1530-1542.
20. Bray NL, Pimentel H, Melsted P and Pachter L. Near-optimal probabilistic RNA-seq quantification. *Nat Biotechnol*. 2016;34:525-7.
21. Soneson C, Love MI and Robinson MD. Differential analyses for RNA-seq: transcript-level estimates improve gene-level inferences. *F1000Res*. 2015;4:1521.
22. Love MI, Huber W and Anders S. Moderated estimation of fold change and dispersion for RNA-seq data with DESeq2. *Genome Biol*. 2014;15:550.
23. Subramanian A, Tamayo P, Mootha VK, Mukherjee S, Ebert BL, Gillette MA, Paulovich A, Pomeroy SL, Golub TR, Lander ES and Mesirov JP. Gene set enrichment analysis: a knowledge-based approach for interpreting genome-wide expression profiles. *Proc Natl Acad Sci U S A*. 2005;102:15545-50.
24. Lei I, West J, Yan Z, Gao X, Fang P, Dennis JH, Gnatovskiy L, Wang W, Kingston RE and Wang Z. BAF250a Protein Regulates Nucleosome Occupancy and Histone Modifications in Priming Embryonic Stem Cell Differentiation. *J Biol Chem*. 2015;290:19343-52.
25. Bodi V, Sanchis J, Morales JM, Marrachelli VG, Nunez J, Forteza MJ, Chaustre F, Gomez C, Mainar L, Minana G, Rumiz E, Husser O, Noguera I, Diaz A, Moratal D, Carratala A, Bosch X, Llacer A, Chorro FJ, Vina JR and Monleon D. Metabolomic profile of human myocardial ischemia by nuclear magnetic resonance spectroscopy of peripheral blood serum: a translational study based on transient coronary occlusion models. *J Am Coll Cardiol*. 2012;59:1629-41.
26. Granger A, Abdullah I, Huebner F, Stout A, Wang T, Huebner T, Epstein JA and Gruber PJ. Histone deacetylase inhibition reduces myocardial ischemia-reperfusion injury in mice. *FASEB J*. 2008;22:3549-60.
27. Frost G, Sleeth ML, Sahuri-Arisoylu M, Lizarbe B, Cerdan S, Brody L, Anastasovska J, Ghourab S, Hankir M, Zhang S, Carling D, Swann JR, Gibson G, Viardot A, Morrison D, Louise Thomas E and Bell JD. The short-chain fatty acid acetate reduces appetite via a central homeostatic mechanism. *Nat Commun*. 2014;5:3611.
28. Gonzalez-Falcon A, Candelario-Jalil E, Garcia-Cabrera M and Leon OS. Effects of pyruvate administration on infarct volume and neurological deficits following permanent focal cerebral ischemia in rats. *Brain Res*. 2003;990:1-7.
29. Vinay P, Lemieux G, Cartier P and Ahmad M. Effect of fatty acids on renal ammoniagenesis in in vivo and in vitro studies. *Am J Physiol*. 1976;231:880-7.
30. MacLellan WR and Schneider MD. Death by design. Programmed cell death in cardiovascular biology and disease. *Circ Res*. 1997;81:137-44.
31. Hausenloy DJ and Yellon DM. Myocardial ischemia-reperfusion injury: a neglected therapeutic target. *J Clin Invest*. 2013;123:92-100.

bioRxiv preprint doi: https://doi.org/10.1101/622746; this version posted April 30, 2019. The copyright holder for this preprint (which was not certified by peer review) is the author/funder, who has granted bioRxiv a license to display the preprint in perpetuity. It is made available under aCC-BY-NC-ND 4.0 International license.

32. Griendling KK, Touyz RM, Zweier JL, Dikalov S, Chilian W, Chen YR, Harrison DG, Bhatnagar A and American Heart Association Council on Basic Cardiovascular S. Measurement of Reactive Oxygen Species, Reactive Nitrogen Species, and Redox-Dependent Signaling in the Cardiovascular System: A Scientific Statement From the American Heart Association. *Circ Res*. 2016;119:e39-75.
33. Fukami T, Iida A, Konishi K and Nakajima M. Human arylacetamide deacetylase hydrolyzes ketoconazole to trigger hepatocellular toxicity. *Biochem Pharmacol*. 2016;116:153-61.
34. Bian F, Kasumov T, Thomas KR, Jobbins KA, David F, Minkler PE, Hoppel CL and Brunengraber H. Peroxisomal and mitochondrial oxidation of fatty acids in the heart, assessed from the 13C labeling of malonyl-CoA and the acetyl moiety of citrate. *J Biol Chem*. 2005;280:9265-71.
35. Shimazu T, Hirschey MD, Newman J, He W, Shirakawa K, Le Moan N, Grueter CA, Lim H, Saunders LR, Stevens RD, Newgard CB, Farese RV, Jr., de Cabo R, Ulrich S, Akassoglou K and Verdin E. Suppression of oxidative stress by beta-hydroxybutyrate, an endogenous histone deacetylase inhibitor. *Science*. 2013;339:211-4.
36. Henry RA, Kuo YM, Bhattacharjee V, Yen TJ and Andrews AJ. Changing the selectivity of p300 by acetyl-CoA modulation of histone acetylation. *ACS Chem Biol*. 2015;10:146-56.
37. Matsubara Y, Kraus JP, Yang-Feng TL, Francke U, Rosenberg LE and Tanaka K. Molecular cloning of cDNAs encoding rat and human medium-chain acyl-CoA dehydrogenase and assignment of the gene to human chromosome 1. *Proc Natl Acad Sci U S A*. 1986;83:6543-7.
38. Jin Q, Yu LR, Wang L, Zhang Z, Kasper LH, Lee JE, Wang C, Brindle PK, Dent SY and Ge K. Distinct roles of GCN5/PCAF-mediated H3K9ac and CBP/p300-mediated H3K18/27ac in nuclear receptor transactivation. *EMBO J*. 2011;30:249-62.
39. Wang Y, Guo YR, Liu K, Yin Z, Liu R, Xia Y, Tan L, Yang P, Lee JH, Li XJ, Hawke D, Zheng Y, Qian X, Lyu J, He J, Xing D, Tao YJ and Lu Z. KAT2A coupled with the alpha-KGDH complex acts as a histone H3 succinyltransferase. *Nature*. 2017;552:273-277.
40. Shi S, Liu K, Chen Y, Zhang S, Lin J, Gong C, Jin Q, Yang XJ, Chen R, Ji Z and Han A. Competitive Inhibition of Lysine Acetyltransferase 2B by a Small Motif of the Adenoviral Oncoprotein E1A. *J Biol Chem*. 2016;291:14363-72.
41. Backs J and Olson EN. Control of cardiac growth by histone acetylation/deacetylation. *Circ Res*. 2006;98:15-24.
42. Russell RR, 3rd, Li J, Coven DL, Pypaert M, Zechner C, Palmeri M, Giordano FJ, Mu J, Birnbaum MJ and Young LH. AMP-activated protein kinase mediates ischemic glucose uptake and prevents postischemic cardiac dysfunction, apoptosis, and injury. *J Clin Invest*. 2004;114:495-503.
43. Cao Y, Bojjireddy N, Kim M, Li T, Zhai P, Nagarajan N, Sadoshima J, Palmiter RD and Tian R. Activation of gamma2-AMPK Suppresses Ribosome Biogenesis and Protects Against Myocardial Ischemia/Reperfusion Injury. *Circ Res*. 2017;121:1182-1191.
44. Salminen A, Kauppinen A and Kaarniranta K. AMPK/Snf1 signaling regulates histone acetylation: Impact on gene expression and epigenetic functions. *Cell Signal*. 2016;28:887-95.
45. Haar L, Ren X, Liu Y, Koch SE, Goines J, Tranter M, Engevik MA, Nieman M, Rubinstein J and Jones WK. Acute consumption of a high-fat diet prior to ischemia-reperfusion results in

bioRxiv preprint doi: https://doi.org/10.1101/622746; this version posted April 30, 2019. The copyright holder for this preprint (which was not certified by peer review) is the author/funder, who has granted bioRxiv a license to display the preprint in perpetuity. It is made available under aCC-BY-NC-ND 4.0 International license.

cardioprotection through NF-kappaB-dependent regulation of autophagic pathways. *Am J Physiol Heart Circ Physiol*. 2014;307:H1705-13.

46. Olenchock BA, Moslehi J, Baik AH, Davidson SM, Williams J, Gibson WJ, Chakraborty AA, Pierce KA, Miller CM, Hanse EA, Kelekar A, Sullivan LB, Wagers AJ, Clish CB, Vander Heiden MG and Kaelin WG, Jr. EGLN1 Inhibition and Rerouting of alpha-Ketoglutarate Suffice for Remote Ischemic Protection. *Cell*. 2016;164:884-95.

47. Chouchani ET, Pell VR, Gaude E, Aksentijevic D, Sundier SY, Robb EL, Logan A, Nadtochiy SM, Ord ENJ, Smith AC, Eyassu F, Shirley R, Hu CH, Dare AJ, James AM, Rogatti S, Hartley RC, Eaton S, Costa ASH, Brookes PS, Davidson SM, Duchen MR, Saeb-Parsy K, Shattock MJ, Robinson AJ, Work LM, Frezza C, Krieg T and Murphy MP. Ischaemic accumulation of succinate controls reperfusion injury through mitochondrial ROS. *Nature*. 2014;515:431-435.

48. Zhang J, Wang YT, Miller JH, Day MM, Munger JC and Brookes PS. Accumulation of Succinate in Cardiac Ischemia Primarily Occurs via Canonical Krebs Cycle Activity. *Cell Rep*. 2018;23:2617-2628.

Figure 1

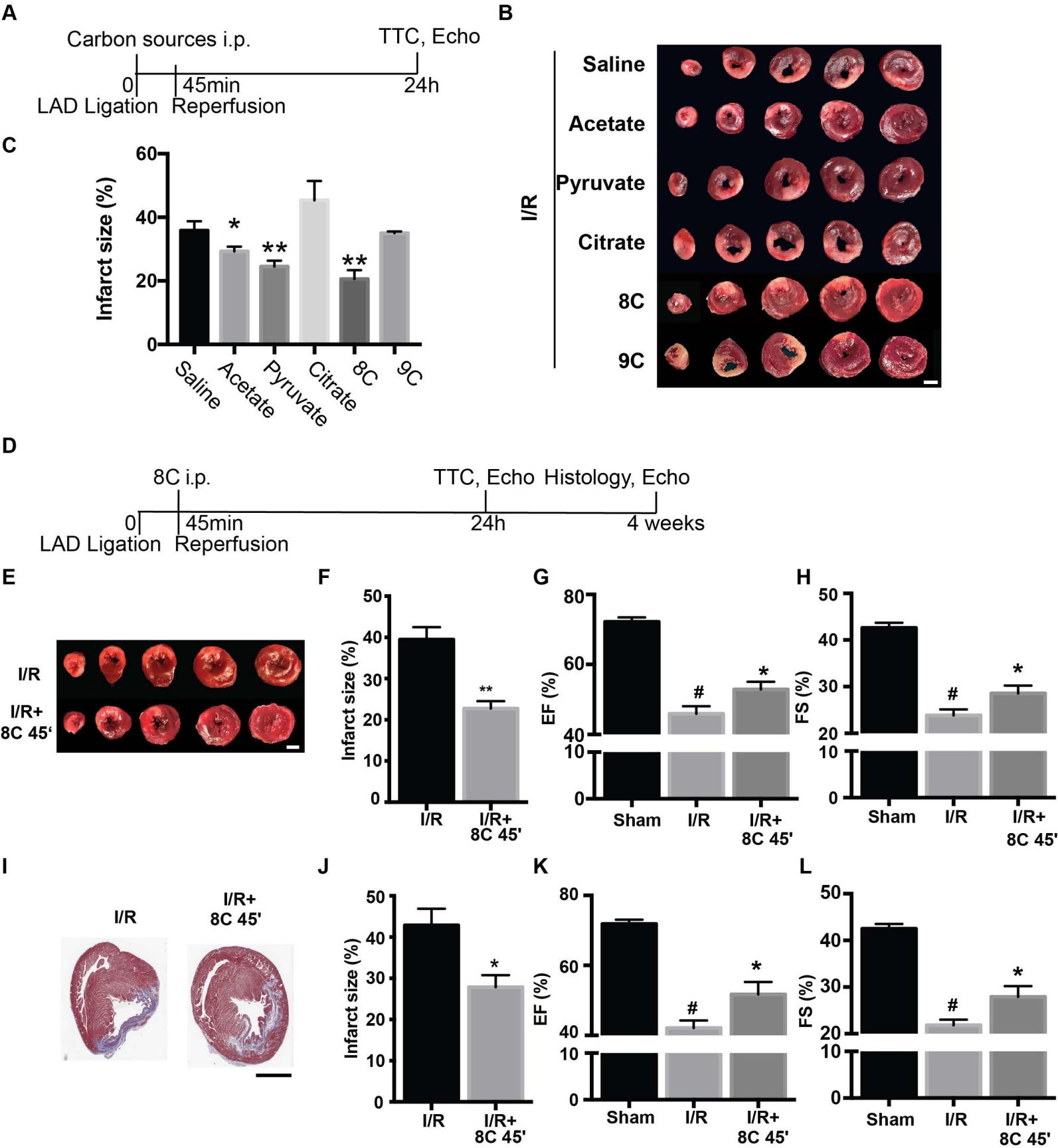
A
Carbon sources i.p.
TTC, Echo
0
45min
24h
LAD Ligation
Reperfusion
B
I/R
Saline
Acetate
Pyruvate
Citrate
8C
9C
C
Infarct size (%)
60
40
20
0
*
**
**
Saline
Acetate
Pyruvate
Citrate
8C
9C
D
8C i.p.
TTC, Echo
Histology, Echo
0
45min
24h
4 weeks
LAD Ligation
Reperfusion
E
I/R
I/R+
8C 45'
F
Infarct size (%)
50
40
30
20
10
0
**
I/R
I/R+
8C 45'
G
EF (%)
80
60
40
10
0
#
*
Sham
I/R
I/R+
8C 45'
H
FS (%)
50
40
30
20
10
0
#
*
Sham
I/R
I/R+
8C 45'
I
I/R
I/R+
8C 45'
J
Infarct size (%)
50
40
30
20
10
0
*
I/R
I/R+
8C 45'
K
EF (%)
80
60
40
10
0
#
*
Sham
I/R
I/R+
8C 45'
L
FS (%)
50
40
30
20
10
0
#
*
Sham
I/R
I/R+
8C 45'

Figure 2

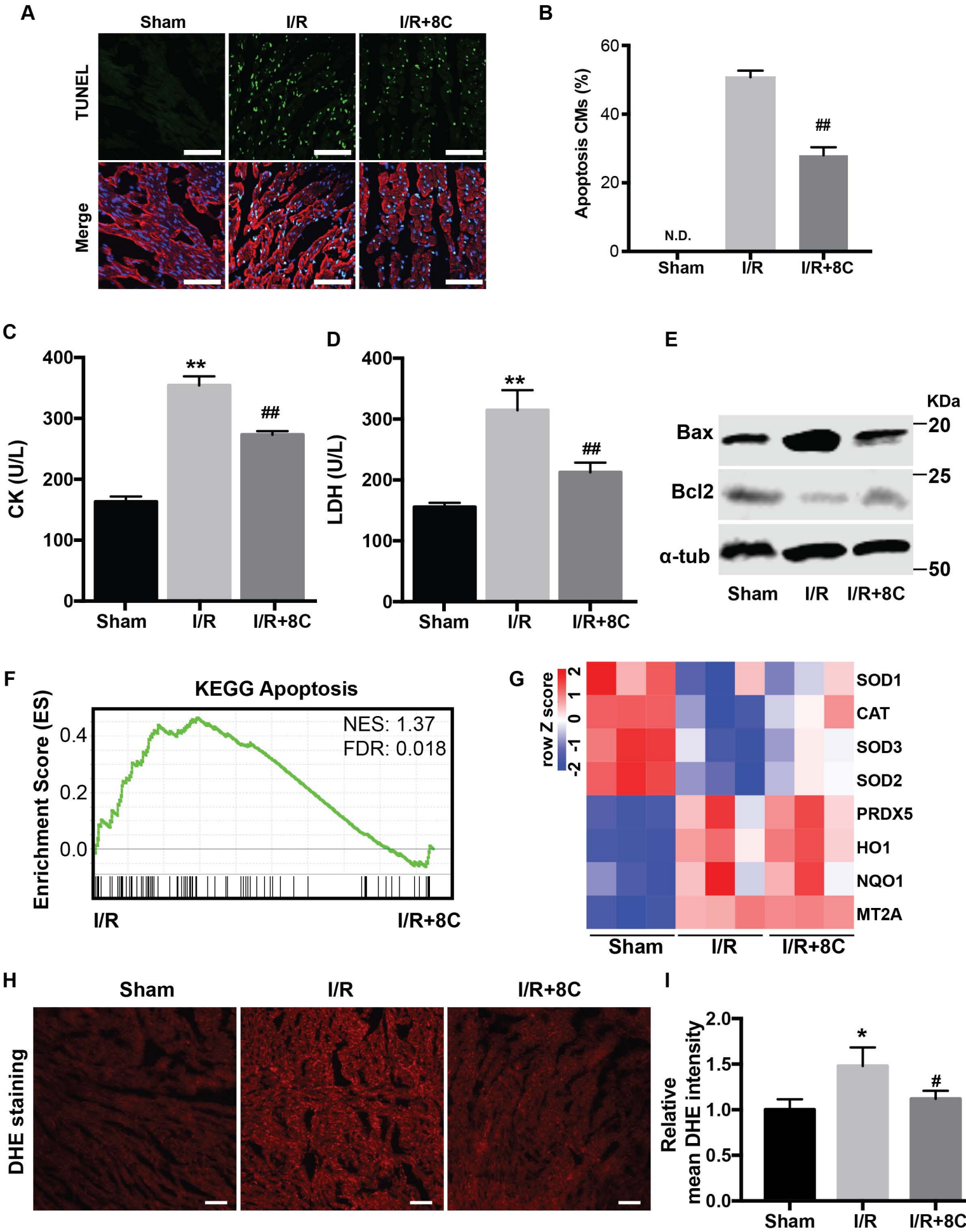
A
Sham
I/R
I/R+8C
TUNEL
Merge
B
Apoptosis CMs (%)
60
40
20
0
N.D.
##
Sham
I/R
I/R+8C
C
CK (U/L)
400
300
200
100
0
**
##
Sham
I/R
I/R+8C
D
LDH (U/L)
400
300
200
100
0
**
##
Sham
I/R
I/R+8C
E
KDa
Bax
Bcl2
α-tub
20
25
50
Sham
I/R
I/R+8C
F
KEGG Apoptosis
Enrichment Score (ES)
0.4
0.2
0.0
NES: 1.37
FDR: 0.018
I/R
I/R+8C
G
row Z score
2
1
0
-1
-2
SOD1
CAT
SOD3
SOD2
PRDX5
HO1
NQO1
MT2A
Sham
I/R
I/R+8C
H
Sham
I/R
I/R+8C
DHE staining
I
Relative mean DHE intensity
2.0
1.5
1.0
0.5
0.0
*
#
Sham
I/R
I/R+8C

Figure 3

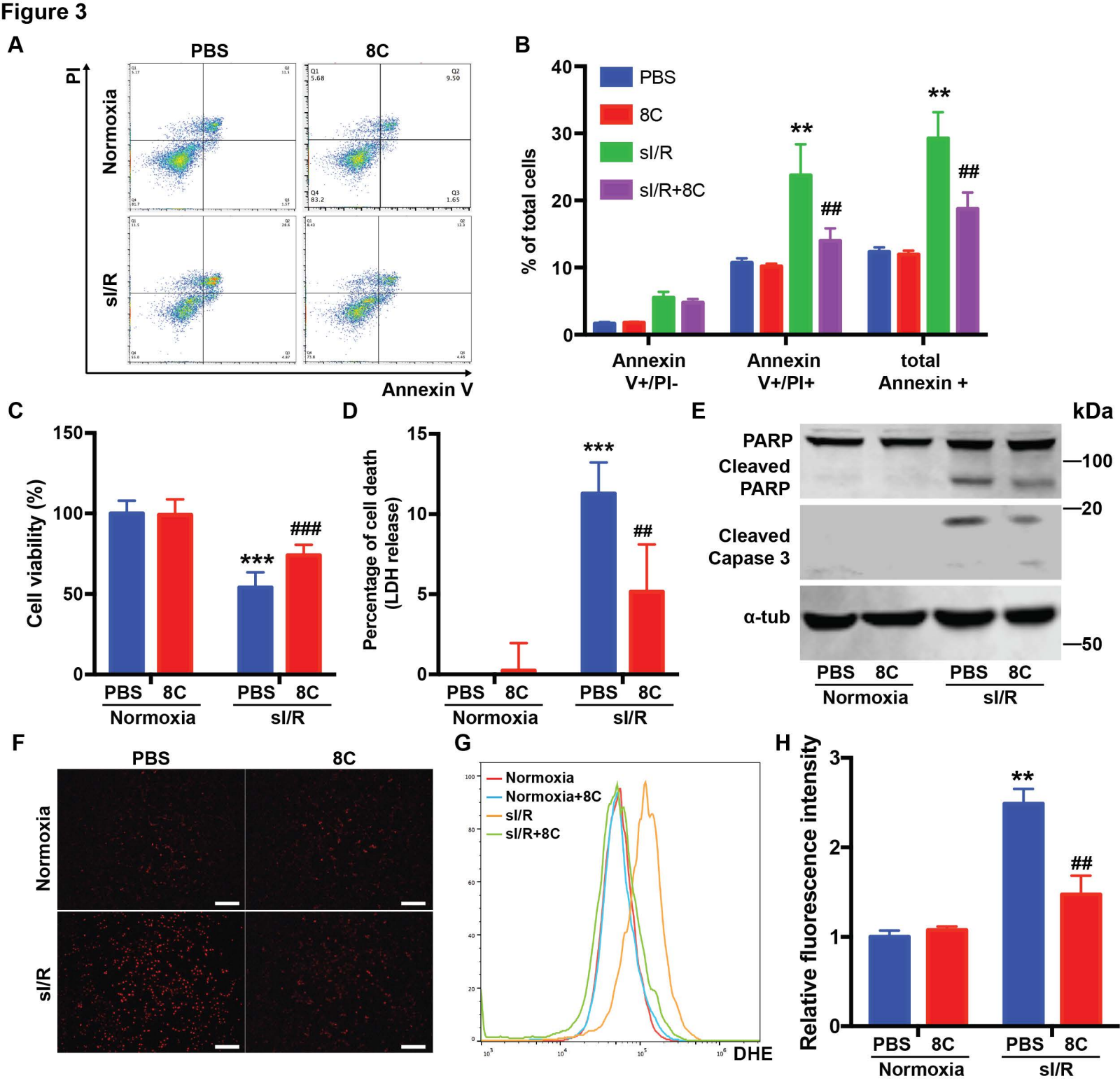
A
PBS
8C
PI
Normoxia
sI/R
Annexin V
B
PBS
8C
sI/R
sI/R+8C
% of total cells
Annexin V+/PI-
Annexin V+/PI+
total Annexin +
C
Cell viability (%)
PBS
8C
Normoxia
sI/R
D
Percentage of cell death (LDH release)
E
kDa
PARP
Cleaved PARP
Cleaved Capase 3
α-tub
F
G
Normoxia
Normoxia+8C
sI/R
sI/R+8C
DHE
H
Relative fluorescence intensity

bioRxiv preprint doi: https://doi.org/10.1101/622746; this version posted April 30, 2019. The copyright holder for this preprint (which was not certified by peer review) is the author/funder, who has granted bioRxiv a license to display the preprint in perpetuity. It is made available under aCC-BY-NC-ND 4.0 International license.

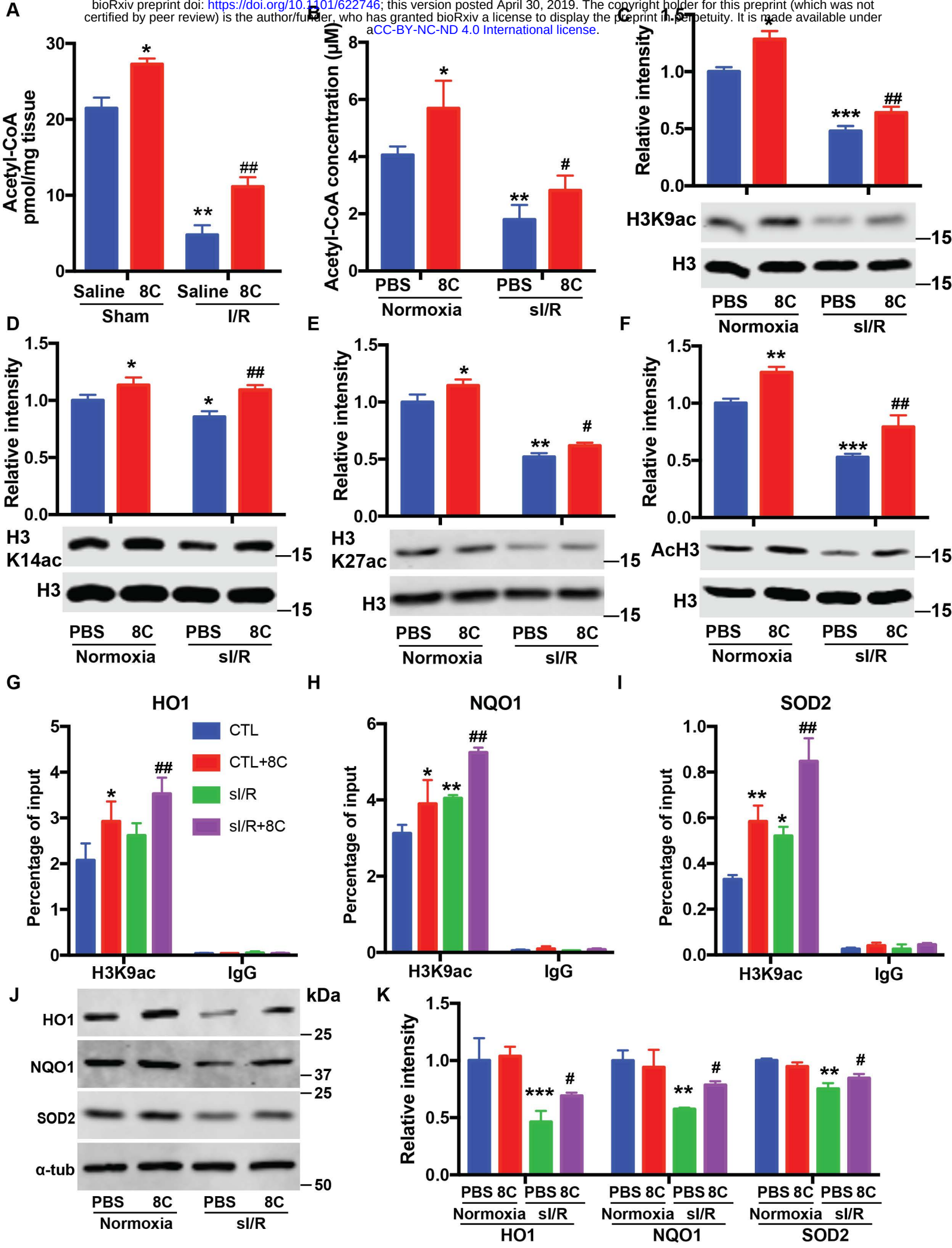

Figure 5

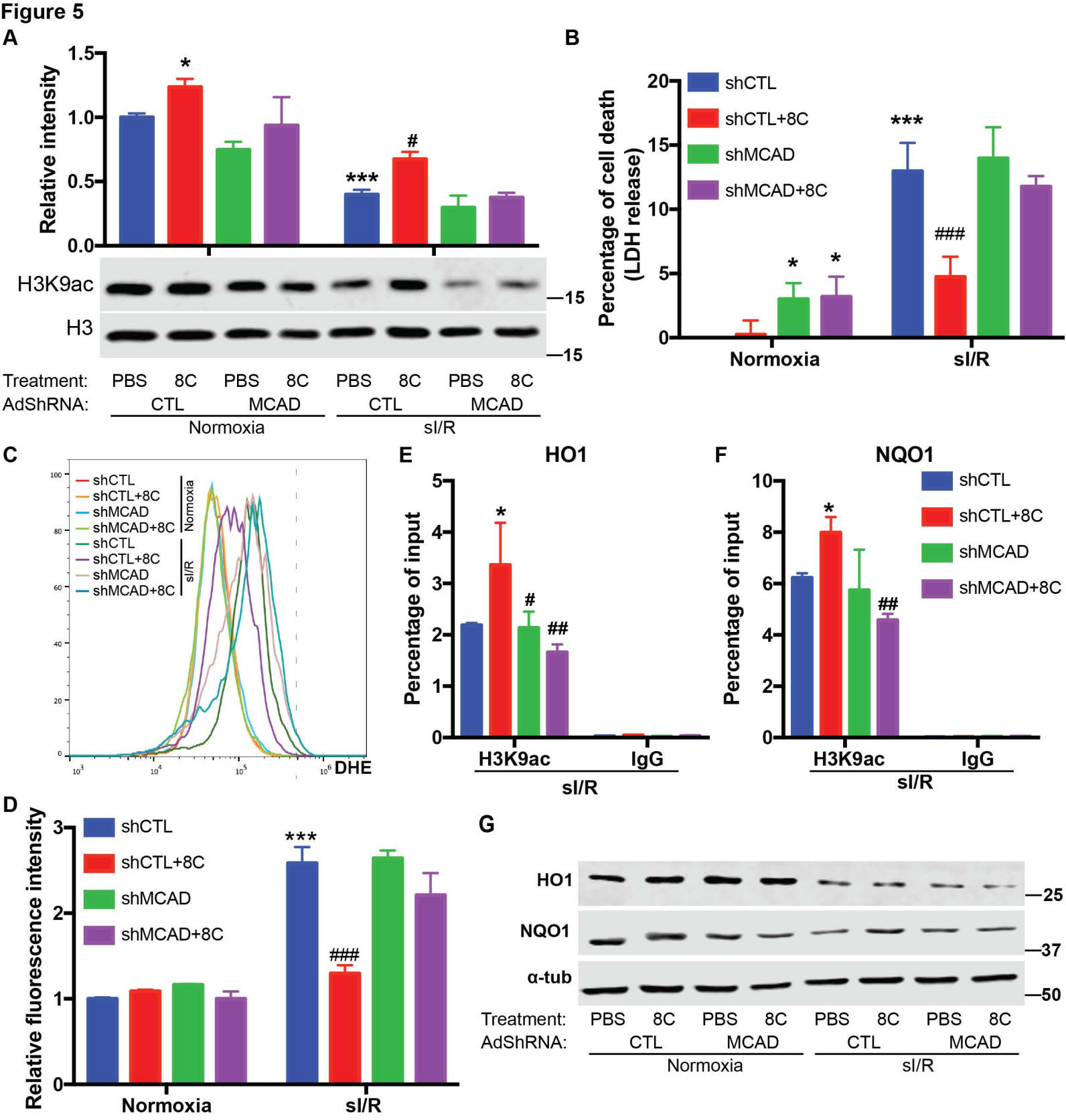
A
Relative intensity
1.5
1.0
0.5
0.0
*
***
#
H3K9ac
H3
15
15
Treatment: PBS 8C PBS 8C PBS 8C PBS 8C
AdShRNA: CTL MCAD CTL MCAD
Normoxia
sI/R
B
Percentage of cell death (LDH release)
20
15
10
5
0
shCTL
shCTL+8C
shMCAD
shMCAD+8C
*
*
***
###
Normoxia
sI/R
C
shCTL
shCTL+8C
shMCAD
shMCAD+8C
Normoxia
shCTL
shCTL+8C
shMCAD
shMCAD+8C
sI/R
DHE
D
Relative fluorescence intensity
3
2
1
0
shCTL
shCTL+8C
shMCAD
shMCAD+8C
***
###
Normoxia
sI/R
E
HO1
Percentage of input
5
4
3
2
1
0
*
#
##
H3K9ac
IgG
sI/R
F
NQO1
Percentage of input
10
8
6
4
2
0
*
##
shCTL
shCTL+8C
shMCAD
shMCAD+8C
H3K9ac
IgG
sI/R
G
HO1
NQO1
α-tub
25
37
50
Treatment: PBS 8C PBS 8C PBS 8C PBS 8C
AdShRNA: CTL MCAD CTL MCAD
Normoxia
sI/R

Figure 6

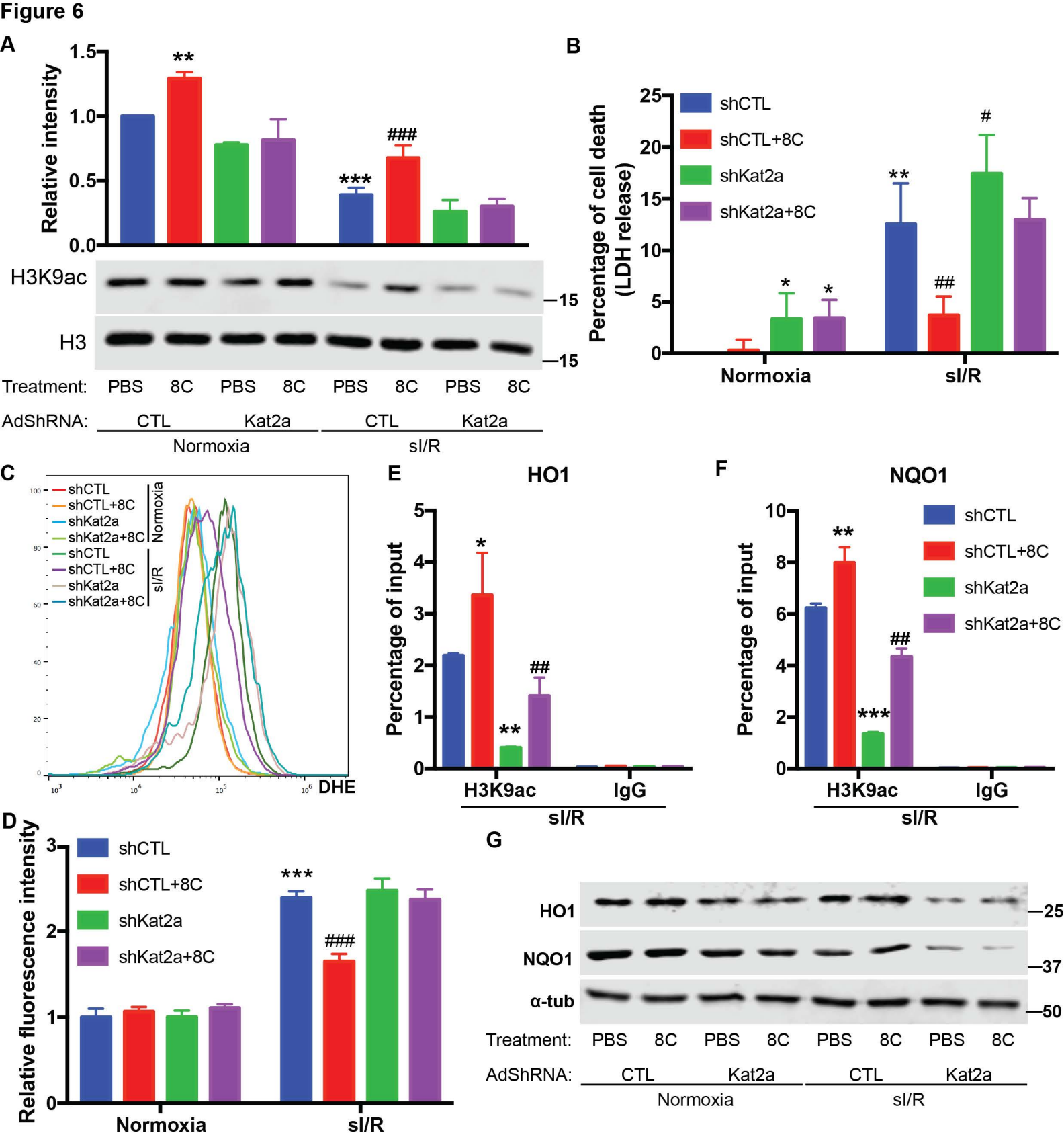
A
Relative intensity
1.5
1.0
0.5
0.0
**
***
###
H3K9ac
H3
15
15
Treatment: PBS 8C PBS 8C PBS 8C PBS 8C
AdShRNA: CTL Kat2a CTL Kat2a
Normoxia
sI/R
B
Percentage of cell death (LDH release)
25
20
15
10
5
0
shCTL
shCTL+8C
shKat2a
shKat2a+8C
*
*
**
##
#
Normoxia
sI/R
C
shCTL
shCTL+8C
shKat2a
shKat2a+8C
Normoxia
shCTL
shCTL+8C
shKat2a
shKat2a+8C
sI/R
100
80
60
40
20
0
10^3
10^4
10^5
10^6
DHE
D
Relative fluorescence intensity
3
2
1
0
shCTL
shCTL+8C
shKat2a
shKat2a+8C
***
###
Normoxia
sI/R
E
HO1
Percentage of input
5
4
3
2
1
0
*
**
##
H3K9ac
IgG
sI/R
F
NQO1
Percentage of input
10
8
6
4
2
0
shCTL
shCTL+8C
shKat2a
shKat2a+8C
**
***
##
H3K9ac
IgG
sI/R
G
HO1
NQO1
α-tub
25
37
50
Treatment: PBS 8C PBS 8C PBS 8C PBS 8C
AdShRNA: CTL Kat2a CTL Kat2a
Normoxia
sI/R